Adaptive Satellite Images Segmentation by Level Set Multiregion Competition

Olfa Besbes, Ziad Belhadj, Nozha Boujemaa

INRIA

INSTITUT NATIONAL DE RECHERCHE EN INFORMATIQUE ET EN AUTOMATIQUE

Adaptive Satellite Images Segmentation by Level Set Multiregion Competition

Olfa Besbes — Ziad Belhadj — Nozha Boujemaa

N° 5855

March 2006

Thème COG

ISSN 0249-6399 ISRN INRIA/RR--5855--FR+ENG

INRIA
ROCQUENCOURT

Adaptive Satellite Images Segmentation by Level Set Multiregion Competition*

Olfa Besbes † ‡, Ziad Belhadj ‡ , Nozha Boujemaa †

Thème COG — Systèmes cognitifs
Projet IMEDIA

Rapport de recherche n° 5855 — March 2006 — 19 pages

Abstract: In this paper, we present an adaptive variational segmentation algorithm of spectral-texture regions in satellite images using level set. Satellite images contain both textured and non-textured regions, so for each region cues of spectral and texture are integrated according to their discrimination power. Motivated by Fisher-Rao's linear discriminant analysis, two region's weights are defined to code respectively the relevance of spectral and texture cues. Therefore, regions with or without texture are processed in the same framework. The obtained segmentation criterion is minimized via curves evolution within an explicit correspondence between the interiors of evolving curves and regions in segmentation. Thus, an unambiguous segmentation to a given arbitrary number of regions is obtained by the multiregion competition algorithm. Experimental results on both natural and satellite images are shown.

Key-words: Level set theory, adaptive multispectral image segmentation, textured / non-textured regions, discrimination power, multiregion competition.

* This work is partially supported by QuerySat project and INRIA STIC project.

† Projet IMEDIA, bat. 11, INRIA Rocquencourt, Domaine de Voluceau, B.P. 105, 78153 Le Chesnay Cedex France, *{Olfa.Besbes, Nozha.Boujemaa}@inria.fr*

‡ Unité URISA, École Supérieure des Communications de Tunis (SUP'COM), Cité Technologique des Communications de Tunis, 2088 Tunisie, *ziad.belhadj@supcom.rnu.tn*

Unité de recherche INRIA Rocquencourt
Domaine de Voluceau, Rocquencourt, BP 105, 78153 Le Chesnay Cedex (France)
Téléphone : +33 1 39 63 55 11 —Télécopie : +33 1 39 63 53 30

Segmentation adaptative d'images satellitaires par courbes de niveaux et compétition multirégion

Résumé : Dans ce rapport, nous proposons un algorithme de segmentation adaptative d'images satellitaires en utilisant une approche variationnelle par courbes de niveaux. Les images satellitaires contiennent des régions texturées et d'autres non texturées. De ce fait, les caractéristiques spectrale et texturale associées à chaque région sont intégrées selon leurs pouvoirs de discrimination. En se basant sur l'analyse de discrimination linéaire de Fisher-Rao, nous définissons pour chaque région deux poids qui codent respectivement la pertience des caractéristiques spectrale et texturale. Ainsi, les régions avec ou sans texture sont analysées dans un même formalisme. Le critère de segmentation obtenu est minimisé par évolution des courbes avec une correspondance explicite entre les régions de la partition et les régions définies par les courbes actives. Une partition du domaine de l'image en un nombre donné quelconque de régions est alors obtenue par l'algorithme de compétition multirégion. Des résultats expérimentaux obtenus sur des images naturelles et satellitaires sont montrés.

Mots-clés : Théorie des courbes de niveaux, segmentation adaptative d'images multi-spectrales, régions texturées / non-texturées, pouvoir de discrimination, compétition multi-région.

1 Introduction

1.1 Problem Statement

The development and application of various remote sensing platforms result in the production of huge amounts of satellite image data. Therefore, there is an increasing need for effective querying and browsing in these image databases. Region-Based Image Retrieval (RBIR) [1] is a powerful tool since it allows to search images containing similar objects of a reference image. It requires the satellite image to be segmented into a number of regions. Segmentation consists in partitioning the image into non-overlapping regions that are homogeneous with regards to some characteristics such as spectral and texture. Remote sensed images contain both textured and non-textured regions. This is even more true today with high resolution images such as IKONOS, SPOT-5 and QuickBird data. In this paper, we propose an adaptive variational segmentation framework for spectral-texture images using active curves evolution via level set [2]. Inspired from [3, 4, 5], we apply a multi-dimensional statistical model to describe regions. In order to cope with content heterogeneity of remote sensed data, we evaluate spectral and texture features relevance according to each region in the image. Furthermore, we use level set multiregion competition algorithm [6] to guarantee a segmentation that is a partition of the image domain into N fixed but arbitrary regions.
The remainder of the paper is organized as follows: Subsection 1.2 is a survey of related works on color (or intensity) / texture image segmentation. Section 2 details our adaptive variational segmentation method. Section 3 presents curve evolution equations and level set implementation. Experimental results for both natural and satellite images are shown in Section 4. We conclude this paper in Section 5.

1.2 Related Works

Different segmentation methods have been developed to deal with natural images having both textured and non-textured regions such as normalized cut [7], JSEG [8], Edgeflow [9, 10] and variational image decomposition [11]. In [7], the gray-level image is analyzed using the two cues of contour and texture in a graph partitioning framework. A local measure of texturedness gates each cue contribution. In [8], the JSEG method consists of two independent steps: color quantization and spatial region growing segmentation. It proposes a notion of J-image to measure the confidence of pixels to be boundaries or interiors of color-texture regions. This method is limited by the color segmentation since it depends on color regions discrimination. The Edgeflow method utilizes a predictive coding model to identify the direction of change in color/texture features and construct an edge flow vector. In [9], three steps are performed to obtain final segmented images: boundary detection, boundary connection and region merging. However, in [10] the segmentation is performed efficiently by integrating edge flow vector field to the curve evolution. The main limitation of Edgeflow-based segmentation is scale parameter selection. A fixed global scale is inappropriate for images which contain multiple scale information. To detect meaningful boundaries in these images, a local scale parameter depending on the local color/texture

properties is required. Moreover, the common drawback of these edge-based methods is the over-segmentation result. In [11], a region-based variational image segmentation algorithm is presented. It's based on image decomposition into a geometrical component and a textured component. The segmentation is carried out by combining the information from both channels with a logical framework. This approach is restricted to gray-level images. Besides, its results depend on the reliability of image decomposition and the supervised definition of the region's logical model.
The above methods seek to provide an unified framework that enables natural images segmentation based on cue combination such as contour, texture and color. This idea of cue-combination has also been used in variational approaches to cope with texture images. In [3], a supervised variational texture segmentation framework was developed. In an off-line step, a global multi-vector statistical model was generated for each texture prototype. A constant weight was determined for each texture feature by a classification result method. This weight codes the power discrimination of its corresponding texture feature. In an on-line step, the segmentation was performed via contour propagation guided by both boundary and region forces. In [5], a non-linear structure tensor was computed as texture features to cope with an active unsupervised gray or color texture segmentation. Unlike features obtained by Gabor filters [3, 12, 13], this approach naturally leads to a significantly reduced number of feature channels. Then, a two-texture segmentation model based on a variational formulation and on the level set representation was applied. A multi-dimensional Gaussian was assumed to approximate region information of the feature channels. These probability density functions were estimated dynamically during the segmentation process. In [14], a TV flow based local scale feature was added to complete this framework. A generalization to multiple region segmentation was proposed in [15].
In the basic framework [5], texture and color cues were combined similarly. Therefore, it can't deal with natural images containing both textured and non-textured regions. In fact, color and texture features have different discrimination power according to the region kind. To deal with such images, we propose an adaptive variational multiregion segmentation approach where spectral (or color) / texture features relevance is considered in the energy functional. The idea of our method is as following: For a non-textured region, color is the most discriminant information since non-textured regions have similar response in the texture feature space. On the other hand, for a textured region we evaluate the coherence between spectral and texture cues in order to discriminate it from others regions in the image.

2 Adaptive Multiple Region Segmentation

Let $I:\Omega\rightarrow\mathbb{R}^C$ be the multispectral image to be segmented, defined on $\Omega\subset\mathbb{R}^2$. $C\geq 1$ is the spectral bands number. We aim to find a partition of this image into N fixed but arbitrary homogeneous regions with respect to spectral and texture characteristics. Let $\Re=\{R_i\}_{i=1}^N$ be a partition of Ω such that $\cup_{i=1}^N R_i=\Omega$ and $R_i\cap R_k=\emptyset$, if $i\neq k$.

2.1 Energy Functional

Following the idea of multi-cue integration in [5], let $\mathbf{U}:\Omega\rightarrow\mathbb{R}^M$ be the computed feature vector of the image I. It consists of C spectral channels and 4 texture features where a coupled edge preserving smoothing process is applied. This so-called nonlinear diffusion [16] deals with outliers in the data, closes structures and synchronises all channels in order to facilitate the segmentation process. The texture features are given by the second order matrix and the local scale feature. The latter is deduced from the speed of a diffusion process based on the TV flow [14]. The resultant feature vector $\mathbf{U}$ describes each region by its spectral (or color) property, the magnitude, the orientation and the local scale of its texture. In figure 1, the feature vector components for a panchromatic satellite image are shown. Let $p_{ij}(x)$ be the conditional probability density function of a value $\mathbf{U}_j(x)$ to be in

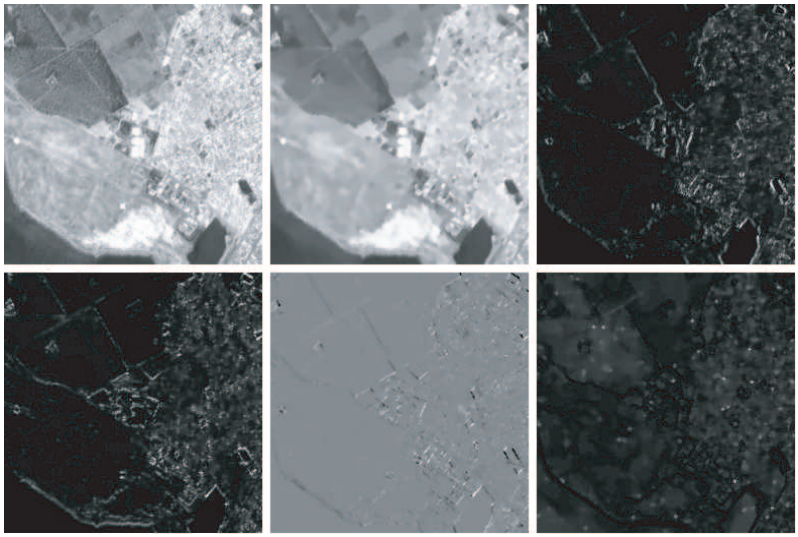

Figure 1: FROM LEFT TO RIGHT, TOP TO BOTTOM: Original image and its feature channels (spectral feature, nonlinear structure tensor components and local scale feature).

a region R_i. The feature channels are assumed to be independent. Assuming all partitions to be equally probable and the pixels within each region to be independent, the adaptive segmentation problem consists of finding the partition $\hat{\Re}$ that minimizes the following energy functional :

$$E(\Re) = -\sum_{i=1}^{N}\int_{R_i} w_{is}\sum_{j=1}^{C}\log p_{ij}(\mathbf{U}_j(x))\,dx + \int_{R_i} w_{it}\sum_{j=C+1}^{M}\log p_{ij}(\mathbf{U}_j(x))\,dx, \qquad (1)$$

where w_{is} and w_{it} are two weights which code respectively the discrimination power of spectral features and texture features in each region R_i. Thanks to this new cost function, we ensure an adaptive segmentation method that deals with images without texture, images

with only textured regions and general images that contain regions of both kinds. Using a Gaussian approximation for all feature channels to model the statistics of each region, we obtain the following energy functional:

$$\begin{aligned} E(\Re) \quad &= \sum_{i=1}^{N} \int_{R_i} w_{is} \sum_{j=1}^{C} \left(\log\left(2\Pi\sigma_{ij}^2\right) + \frac{\left(\mathbf{U}_j(x)-\mu_{ij}\right)^2}{\sigma_{ij}^2} \right) dx \\ &+ \int_{R_i} w_{it} \sum_{j=C+1}^{M} \left(\log\left(2\Pi\sigma_{ij}^2\right) + \frac{\left(\mathbf{U}_j(x)-\mu_{ij}\right)^2}{\sigma_{ij}^2} \right) dx \end{aligned} \quad . \tag{2}$$

2.2 Defining Region Weights

We use the well-known Fisher-Rao statistical criterion [17, 18], to determine the different weights $\{w_{is}, w_{it}\}_{i=1}^{N}$. It consists on maximizing the ratio of the between-class variance $\mathbf{B}$ to the within-class variance $\mathbf{W}$ in any particular data set thereby guaranteeing maximal separability. This linear discrimination technique has widely used for feature space dimensionality reduction [19]. A generalization into kernel version was developed for nonlinear discriminative analysis [20, 21]. For N-classes case, $\mathbf{B}$ and $\mathbf{W}$ are defined below:

$$\mathbf{B} = \sum_{i=1}^{N-1} \sum_{k=i+1}^{N} p_i p_k \left(\mu_i - \mu_k\right)\left(\mu_i - \mu_k\right)^T \qquad \mathbf{W} = \sum_{i=1}^{N} p_i \mathbf{W_i}, \tag{3}$$

where μ_i is is the mean vector of class i, p_i is its *a priori* probability and $\mathbf{W_i}$ is its within-class covariance. Assuming equally probable regions, p_i equals $\frac{1}{N}$. For a defined feature space, the $\mathbf{W^{-1}B}$ eigenvalues code the relevance of their corresponding feature channels. Furthermore, $trace(\mathbf{W^{-1}B})$ measures the feature space relevance. The higher value of this inter-intra criterion, the more informative is the feature space. In order to measure the relevance of a feature space to discriminate a given region R_i from others regions $R_{k|k\neq i}$, we only consider R_i's between-class variance. Therefore, we define $\mathbf{B_i}$ as follows:

$$\mathbf{B_i} = \frac{1}{N^2} \sum_{k=1|k\neq i}^{N} \left(\mu_i - \mu_k\right)\left(\mu_i - \mu_k\right)^T. \tag{4}$$

Then spectral and texture weights of a region R_i can be written as :

$$w_{is} = \frac{\sum_{j=1}^{C} \left[\mathbf{W^{-1}B_i}\right]_{jj}}{\sum_{j=1}^{M} \left[\mathbf{W^{-1}B_i}\right]_{jj}} \qquad w_{it} = \frac{\sum_{j=C+1}^{M} \left[\mathbf{W^{-1}B_i}\right]_{jj}}{\sum_{j=1}^{M} \left[\mathbf{W^{-1}B_i}\right]_{jj}}, \tag{5}$$

where:

$$\left[\mathbf{W^{-1}B_i}\right]_{jj} = \frac{\sum_{k=1}^{N} \left(\mu_{ij} - \mu_{kj}\right)^2}{N \sum_{k=1}^{N} \sigma_{kj}^2}. \tag{6}$$

Noting that $\{w_{is}, w_{it}\} \in [0,1]$ and $w_{is} + w_{it} = 1, \forall i \in [1, N]$.

2.3 Representation of a Partition

In order to find the partition $\hat{\Re} = \left\{\hat{R}_i\right\}_{i=1}^{N}$ that minimizes the energy functional (2), we use active curves evolution. We consider a family $\overrightarrow{\gamma}_i : [0,1] \to \Omega, i = 1, \ldots, N-1$ of plane curves parameterized by the arc parameter $s \in [0,1]$. As proposed in [6], we use the following explicit correspondence between the regions $R_{\overrightarrow{\gamma}_i}$ enclosed by curves $\overrightarrow{\gamma}_i$ and the regions of the partition $\Re = \{R_i\}_{i\in[1,N]}$ are:

$$\begin{aligned}
&R_1 = R_{\overrightarrow{\gamma}_1} \\
&R_2 = R^c_{\overrightarrow{\gamma}_1} \cap R_{\overrightarrow{\gamma}_2} \\
&\ldots \\
&R_k = R^c_{\overrightarrow{\gamma}_1} \cap R^c_{\overrightarrow{\gamma}_2} \cap \ldots \cap R^c_{\overrightarrow{\gamma}_{k-1}} \cap R_{\overrightarrow{\gamma}_k} \\
&\ldots \\
&R_N = R^c_{\overrightarrow{\gamma}_1} \cap R^c_{\overrightarrow{\gamma}_2} \cap \ldots \cap R^c_{\overrightarrow{\gamma}_{N-2}} \cap R^c_{\overrightarrow{\gamma}_{N-1}}
\end{aligned} \quad . \tag{7}$$

The partition representation for four regions is shown in figure 2. This representation guarantees an unambiguous image segmentation to N arbitrary number of regions without adding a constraint term to energy functional [3, 22]. With this choice of representing an image domain partition and with a regularization term related to the length of curves addition, the energy functional (2) becomes:

$$\begin{aligned}
E\left(\{R_i\}_{i=1}^{N}\right) \quad &= \int_{R_{\overrightarrow{\gamma}_1}} \xi_1(x)\,dx + \int_{R^c_{\overrightarrow{\gamma}_1} \cap R_{\overrightarrow{\gamma}_2}} \xi_2(x)\,dx + \ldots \\
&+ \int_{R^c_{\overrightarrow{\gamma}_1} \cap R^c_{\overrightarrow{\gamma}_2} \cap \ldots \cap R^c_{\overrightarrow{\gamma}_{k-1}} \cap R_{\overrightarrow{\gamma}_k}} \xi_k(x)\,dx + \ldots \\
&+ \int_{R^c_{\overrightarrow{\gamma}_1} \cap R^c_{\overrightarrow{\gamma}_2} \cap \ldots \cap R^c_{\overrightarrow{\gamma}_{N-2}} \cap R^c_{\overrightarrow{\gamma}_{N-1}}} \xi_N(x)\,dx \\
&+ \lambda \sum_{i=1}^{N-1} \oint_{\overrightarrow{\gamma}_i} ds,
\end{aligned} \tag{8}$$

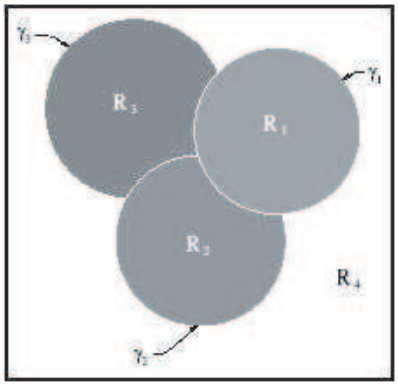

Figure 2: Representation of a partition.

where λ is a positive real constant to weight the contribution of the regularization term. For each region R_i, we have $\xi_i(x) = w_{is}\xi_{is}(x) + w_{it}\xi_{it}(x)$, where :
$\xi_{is}(x) = \sum_{j=1}^{C}\Big(\log\big(2\Pi\sigma_{ij}^2\big) + \frac{(\mathbf{U}_j(x)-\mu_{ij})^2}{\sigma_{ij}^2}\Big)$ and $\xi_{it}(x) = \sum_{j=C+1}^{M}\Big(\log\big(2\Pi\sigma_{ij}^2\big) + \frac{(\mathbf{U}_j(x)-\mu_{ij})^2}{\sigma_{ij}^2}\Big)$.

3 Segmentation by Curves Evolution

3.1 Curve Evolution Equations

The energy functional (8) minimum is obtained via the gradient descent with respect to the curves position. We directly differentiate this functional using the shape derivative tool introduced in [23]. First, we consider 2-phase case. Then, we present the system of curves evolution equations in the case of multiple-region segmentation.

3.1.1 Tow-Region Segmentation

For segmentation into two regions, we minimize the following criterion :

$$E(R_1, R_2) = \int_{R_{\overrightarrow{\gamma}_1}} \xi_1(x)dx + \int_{R^c_{\overrightarrow{\gamma}_1}} \xi_2(x)dx + \lambda \oint_{\overrightarrow{\gamma}_1} ds. \tag{9}$$

We estimate the statistical parameters as follows :

$$\begin{cases} \mu_{1j} = \frac{\int_{R_{\overrightarrow{\gamma}_1}} \mathbf{U}_j(x)dx}{|R_1|} & \sigma_{1j}^2 = \frac{\int_{R_{\overrightarrow{\gamma}_1}} \big(\mathbf{U}_j(x)-\mu_{1j}\big)^2 dx}{|R_1|} \\ \mu_{2j} = \frac{\int_{R^c_{\overrightarrow{\gamma}_1}} \mathbf{U}_j(x)dx}{|R_2|} & \sigma_{2j}^2 = \frac{\int_{R^c_{\overrightarrow{\gamma}_1}} \big(\mathbf{U}_j(x)-\mu_{2j}\big)^2 dx}{|R_2|} \end{cases} \quad \forall j = 1, \ldots, M\,, \tag{10}$$

where $|R_1| = \int_{R_{\overrightarrow{\gamma}_1}} dx$ and $|R_2| = \int_{R^c_{\overrightarrow{\gamma}_1}} dx$ are region areas. As defined in (5), (6), the R_1 and R_2 spectral (respectively textural) weights are equal for 2-region segmentation and we have the following equalities :

$$w_{1s} = w_{2s} = \frac{\sum_{j=1}^{C} Z_j}{\sum_{j=1}^{M} Z_j} \qquad w_{1t} = w_{2t} = \frac{\sum_{j=C+1}^{M} Z_j}{\sum_{j=1}^{M} Z_j}, \tag{11}$$

where $Z_j = \frac{(\mu_{1j}-\mu_{2j})^2}{\sigma_{1j}^2+\sigma_{2j}^2}$. Following [23], we compute the Gâteaux derivative of region functional $D_1 = \int_{R_{\overrightarrow{\gamma}_1}} \xi_1(x)dx$ (respectively $D_2 = \int_{R^c_{\overrightarrow{\gamma}_1}} \xi_2(x)dx$) in the direction of V :

$$\big\langle D_1', V\big\rangle = \int_{R_{\overrightarrow{\gamma}_1}} \xi_1^{sh}\big(x, R_{\overrightarrow{\gamma}_1}, V\big)\, dx - \int_{\overrightarrow{\gamma}_1} \xi_1(x)\,\big(V(x)\,.N_1(x)\big)\, da(x)\,, \tag{12}$$

where $N_1(x)$ is the unit normal vector to the curve $\overrightarrow{\gamma}_1$ at a point x. ξ_1^{sh} is the shape derivative of ξ_1 :

$$\begin{aligned}\xi_1^{sh}\left(x, R_{\overrightarrow{\gamma}_1}, V\right) &= \left[w_{1s}\xi_{1s}(x) + w_{1t}\xi_{1t}(x)\right]^{sh} \\ &= \xi_{1s}(x)\left\langle (w_{1s})', V\right\rangle + \xi_{1t}(x)\left\langle (w_{1t})', V\right\rangle \\ &+ w_{1s}\sum_{j=1}^{C}\left(\frac{\partial \xi_{1s}}{\partial \mu_{1j}}\left\langle (\mu_{1j})', V\right\rangle + \frac{\partial \xi_{1s}}{\partial \sigma_{1j}^2}\left\langle (\sigma_{1j}^2)', V\right\rangle\right) \\ &+ w_{1t}\sum_{j=C+1}^{M}\left(\frac{\partial \xi_{1t}}{\partial \mu_{1j}}\left\langle (\mu_{1j})', V\right\rangle + \frac{\partial \xi_{1t}}{\partial \sigma_{1j}^2}\left\langle (\sigma_{1j}^2)', V\right\rangle\right)\end{aligned} . \tag{13}$$

Using $\left\langle (w_{1t})', V\right\rangle = -\left\langle (w_{1s})', V\right\rangle$ and after some algebraic manipulation, we obtain:

$$\int_{R_{\overrightarrow{\gamma}_1}} \xi_1^{sh}\left(x, R_{\overrightarrow{\gamma}_1}, V\right) dx = |R_1|\left((2C-M)\left(1+\log(2\Pi)\right) + \sum_{j=1}^{C}\log\left(\sigma_{1j}^2\right) - \sum_{j=C+1}^{M}\log\left(\sigma_{1j}^2\right)\right)\left\langle (w_{1s})', V\right\rangle . \tag{14}$$

Similarly, we compute the Gâteaux derivative of the spectral weight w_{1s} (see the annex) :

$$\left\langle (w_{1s})', V\right\rangle = \frac{1}{\sum_{j=1}^{M} Z_j}\int_{\overrightarrow{\gamma}_1}\left[w_{1t}\sum_{j=1}^{C}k_{1j}(x) - w_{1s}\sum_{j=C+1}^{M}k_{1j}(x)\right]\left(V(x).N_1(x)\right)da(x), \tag{15}$$

where :

$$\begin{aligned}k_{1j}(x) &= 2\frac{\left(\mu_{2j}-\mu_{1j}\right)}{\left(\sigma_{1j}^2+\sigma_{2j}^2\right)}\left(\frac{\left(U_j(x)-\mu_{1j}\right)}{|R_1|} + \frac{\left(U_j(x)-\mu_{2j}\right)}{|R_2|}\right) \\ &+ \frac{\left(\mu_{1j}-\mu_{2j}\right)^2}{\left(\sigma_{1j}^2+\sigma_{2j}^2\right)^2}\left(\frac{\left(U_j(x)-\mu_{1j}\right)^2-\sigma_{1j}^2}{|R_1|} - \frac{\left(U_j(x)-\mu_{2j}\right)^2-\sigma_{2j}^2}{|R_2|}\right)\end{aligned} . \tag{16}$$

Therefore, we get the following region functionals Gâteaux derivative:

$$\left\langle D_i', V\right\rangle = \int_{\overrightarrow{\gamma}_1}\left[A_i\left(w_{it}\sum_{j=1}^{C}k_{ij}(x) - w_{is}\sum_{j=C+1}^{M}k_{ij}(x)\right) + /-\xi_i(x)\right]\left(V(x).N_1(x)\right)da(x), \tag{17}$$

where $k_{1j} = k_{2j}|_{j\in[1,M]}$ and $A_i = \dfrac{|R_i|\left((2C-M)(1+\log(2\Pi)) + \sum_{j=1}^{C}\log\left(\sigma_{ij}^2\right) - \sum_{j=C+1}^{M}\log\left(\sigma_{ij}^2\right)\right)}{\sum_{j=1}^{M} Z_j}$ for $i = 1, 2$.

Now we can write the $\overrightarrow{\gamma}_1$'s evolution equation:

$$\frac{\partial \overrightarrow{\gamma}_1}{\partial t}(x) = -\left[\xi_1(x) - \Psi_1(x) + \lambda\kappa_1\right]N_1, \tag{18}$$

where $\Psi_1(x) = \sum_{i=1}^{2} A_i\left(w_{it}\sum_{j=1}^{C}k_{ij}(x) - w_{is}\sum_{j=C+1}^{M}k_{ij}(x)\right) + \xi_2(x)$ and κ_1 is the mean curvature function of $\overrightarrow{\gamma}_1$.

Figure 3: FROM LEFT TO RIGHT, TOP TO BOTTOM: (a), (c), (e), and (g) Natural images. (b), (d), (f) and (h) their corresponding segmentation results superimposed on original images.

3.1.2 Multiple-Region Segmentation

We solve the minimization of multiple region segmentation criterion (8) by curves evolution $\left\{\frac{\partial \overrightarrow{\gamma}_i}{\partial t}\right\}_{i=1}^{N-1}$. Starting with $\overrightarrow{\gamma}_1$, we rewrite the energy functional (8) as follows:

$$E(\Re) = \int_{R_{\overrightarrow{\gamma}_1}} \xi_1(x)\,dx + \int_{R^c_{\overrightarrow{\gamma}_1}} \phi_1(x)\,dx + \lambda \oint_{\overrightarrow{\gamma}_1} ds + \lambda \sum_{i=2}^{N-1} \oint_{\overrightarrow{\gamma}_i} ds. \tag{19}$$

We define, for $1 \leq i, n \leq N$, $\phi_n(x) = \sum_{i=n+1}^{N} \xi_i(x)\,\chi_i^n(x)$ and χ_i^n as:

$$\begin{cases} \chi_i^n(x) = 0 & \text{if} \quad i < n \\ \chi_i^n(x) = -1 & \text{if} \quad i = n \\ \chi_i^n(x) = \chi_{R^c_{\overrightarrow{\gamma}_{n+1}}}(x) \cdots \chi_{R^c_{\overrightarrow{\gamma}_{i-1}}}(x)\,\chi_{R_{\overrightarrow{\gamma}_i}}(x) & \text{otherwise} \end{cases}. \tag{20}$$

The statistical parameters for $j \in [\![1, M]\!]$ are also rewritten as follows :

$$\begin{array}{ll} \mu_{1j} = \frac{1}{|R_1|} \int_{R_{\overrightarrow{\gamma}_1}} \mathbf{U}_j(x)\,dx & \sigma_{1j}^2 = \frac{1}{|R_1|} \int_{R_{\overrightarrow{\gamma}_1}} (\mathbf{U}_j(x) - \mu_{1j})^2\,dx \\ \mu_{kj} = \frac{1}{|R_k|} \int_{R^c_{\overrightarrow{\gamma}_1}} \mathbf{U}_j(x)\,\chi_k^1(x)\,dx & \sigma_{kj}^2 = \frac{1}{|R_k|} \int_{R^c_{\overrightarrow{\gamma}_1}} (\mathbf{U}_j(x) - \mu_{kj})^2\,\chi_k^1(x)\,dx \end{array}, \tag{21}$$

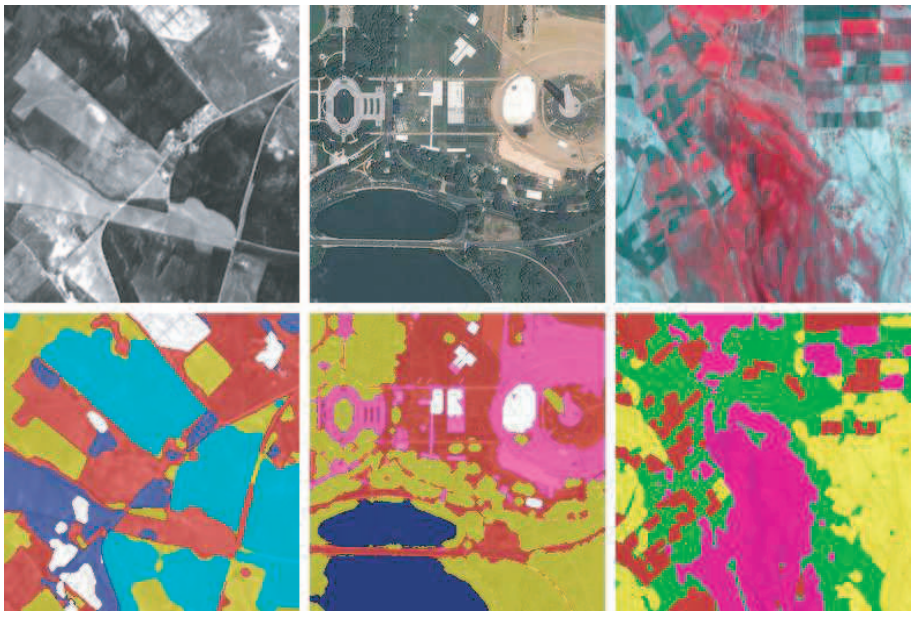

Figure 4: FROM LEFT TO RIGHT, TOP TO BOTTOM: (a), (b) and (c) Original images (256x256) without textured regions. (d), (e) and (f) their corresponding segmentation results superimposed on original images.

where :

$$\begin{array}{ll} |R_1| = \int_{R_{\overrightarrow{\gamma}_1}} dx & \\ \forall k = 2, \ldots, N \qquad & |R_k| = \int_{R^c_{\overrightarrow{\gamma}_1}} \chi^1_k(x)\, dx \end{array} . \tag{22}$$

The spectral and textural weights of R_1 are defined respectively as in (5) and (6):

$$w_{1s} = \frac{\sum_{j=1}^{C} Z_{1j}}{\sum_{j=1}^{M} Z_{1j}} \qquad w_{1t} = \frac{\sum_{j=C+1}^{M} Z_{1j}}{\sum_{j=1}^{M} Z_{1j}}, \tag{23}$$

where $Z_{1j} = \frac{\sum_{i=1}^{N} (\mu_{1j} - \mu_{ij})^2}{\sum_{i=1}^{N} \sigma_{ij}^2}$. Using the result of the annex, we obtain the energy term $\Psi_n(x) =$

$\sum_{i=1}^{N} A_i \left(w_{it} \sum_{j=1}^{C} k_{ij}^n(x) - w_{is} \sum_{j=C+1}^{M} k_{ij}^n(x) \right) + \phi_n(x)$, where $\forall\{i,n\}=\{1,\ldots,N\}$:

$$A_i = \frac{|R_i| \left((2C-M)(1+\log(2\Pi)) + \sum_{j=1}^{C} \log\left(\sigma_{ij}^2\right) - \sum_{j=C+1}^{M} \log\left(\sigma_{ij}^2\right) \right)}{\sum_{j=1}^{M} Z_{\mathrm{ij}}} \tag{24}$$

$$\begin{aligned} \text{and} \quad k_{ij}^n(x) \quad &= \frac{2\left(\mu_{ij}-\mu_{nj}\right)}{\sum_{l=1}^{N} \sigma_{lj}^2} \frac{\mathbf{U}_{j(x)}-\mu_{nj}}{|R_n|} \\ &+ \frac{2}{\sum_{l=1}^{N} \sigma_{lj}^2} \sum_{k=1}^{N} (\mu_{ij}-\mu_{kj}) \frac{\mathbf{U}_{j(x)}-\mu_{ij}}{|R_i|} \chi_i^n(x) \\ &- \frac{2}{\sum_{l=1}^{N} \sigma_{lj}^2} \sum_{k=n+1}^{N} \left[(\mu_{ij}-\mu_{kj}) \frac{\mathbf{U}_{j(x)}-\mu_{kj}}{|R_k|} \chi_k^n(x) \right] \\ &+ \frac{\sum_{k=1}^{N} \left(\mu_{ij}-\mu_{kj}\right)^2}{\left(\sum_{l=1}^{N} \sigma_{lj}^2\right)^2} \left[\frac{\left(\mathbf{U}_{j(x)}-\mu_{nj}\right)^2 - \sigma_{nj}^2}{|R_n|} - \sum_{k=n+1}^{N} \left(\frac{\left(\mathbf{U}_{j(x)}-\mu_{kj}\right)^2 - \sigma_{kj}^2}{|R_k|} \chi_k^n(x) \right) \right] \end{aligned} \tag{25}$$

Furthermore, the $\overrightarrow{\gamma}_1$'s evolution equation is:

$$\frac{\partial \overrightarrow{\gamma}_1}{\partial t}(x) = -\left[\xi_1(x) - \Psi_1(x) + \lambda\kappa_1\right] N_1. \tag{26}$$

As the same manner, we compute the $\overrightarrow{\gamma}_2$'s evolution equation. We consider that $R_{\overrightarrow{\gamma}_1}$ parameters $\left(\left\{\mu_{1j}, \sigma_{1j}^2\right\}_{j\in[1,M]}, |R_1|\right)$ are constant during the evolution of $\overrightarrow{\gamma}_2$. Therefore, we have the following equation:

$$\frac{\partial \overrightarrow{\gamma}_2}{\partial t}(x) = \left[-\chi_{R^c_{\overrightarrow{\gamma}_1}}(x) \left(\xi_2(x) - \Psi_2(x)\right) + \lambda\kappa_2\right] N_2. \tag{27}$$

Proceeding similarly, a curve $\overrightarrow{\gamma}_n$ has the following evolution equation:

$$\frac{\partial \overrightarrow{\gamma}_n}{\partial t}(x) = -[\chi_1^c(x) \ldots \chi_{n-1}^c(x) \left(\xi_n(x) - \Psi_n(x)\right) + \lambda\kappa_n] N_n. \tag{28}$$

Finally, the minimization of the adaptive multiregion competition functional (8) is achieved through the following system of coupled curves evolution equations:

$$\begin{cases} \frac{\partial \overrightarrow{\gamma}_1}{\partial t}(x) = -[\xi_1(x) - \Psi_1(x) + \lambda\kappa_1] N_1 \\ \frac{\partial \overrightarrow{\gamma}_n}{\partial t}(x) = -[\chi_{R^c_{\overrightarrow{\gamma}_1}}(x) \ldots \chi_{R^c_{\overrightarrow{\gamma}_{n-1}}}(x) \left(\xi_n(x) - \Psi_n(x)\right) + \lambda\kappa_n] N_n, \quad . \\ n = 2, \ldots, N-1 \end{cases} \tag{29}$$

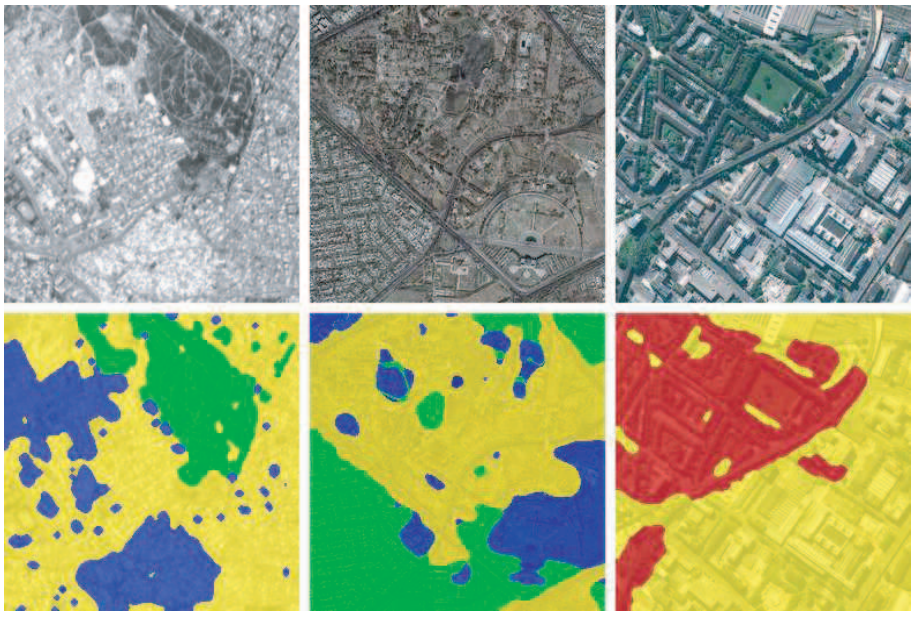

Figure 5: FROM LEFT TO RIGHT, TOP TO BOTTOM: (a), (b) and (c) Original images (256x256) with only textured regions. (d), (e) and (f) their corresponding segmentation results superimposed on original images.

3.2 Level Set Implementation

The system of curves evolution equations (29) is implemented via level set formalism [2]. Thus, the curves $\{\overrightarrow{\gamma}_i\}_{i=1}^{N-1}$ are implicitly represented by the zero level set of a function $u_i : \mathbb{R}^2 \to \mathbb{R}$. The region $R_{\overrightarrow{\gamma}_i}$ inside $\overrightarrow{\gamma}_i$ corresponds to $u_i > 0$. This implicit representation has several advantages. First, the region membership is explicitly maintained. Second, it allows topological changes and can be implemented by stable numerical schemes. The system of curves evolution equations (29) leads to the following system :

$$\begin{cases} \frac{\partial u_1}{\partial t}(x) = -[\xi_1(x) - \Psi_1(x) + \lambda\kappa_{u_1}]\|\overrightarrow{\nabla} u_1\| \\ \frac{\partial u_n}{\partial t}(x) = -[\chi_{\{u_1(x,t)\leq 0\}} \cdots \chi_{\{u_{n-1}(x,t)\leq 0\}} (\xi_n(x) - \Psi_n(x)) + \lambda\kappa_{u_n}]\|\overrightarrow{\nabla} u_n\|, \\ n = 2, \ldots, N-1 \end{cases} \tag{30}$$

where $\chi_{\{u_i(x,t)\leq 0\}} = 1$ if $u_i(x,t) \leq 0$ and 0 otherwise. $\kappa_{u_i} = -div\left(\frac{\overrightarrow{\nabla} u_i}{\|\overrightarrow{\nabla} u_i\|}\right)$ is the u_i's curvature. At convergence, the final segmentation is given by the family $\left\{R_{u_1}, R_{u_1}^c \cap R_{u_2}, \ldots, \cap_{i=1}^{N-1} R_{u_i}^c\right\}$ where $R_{u_i} = \{x \in \Omega \,|\, u_i(x,\infty) > 0\}$, $i = 1, \ldots, N-1$.

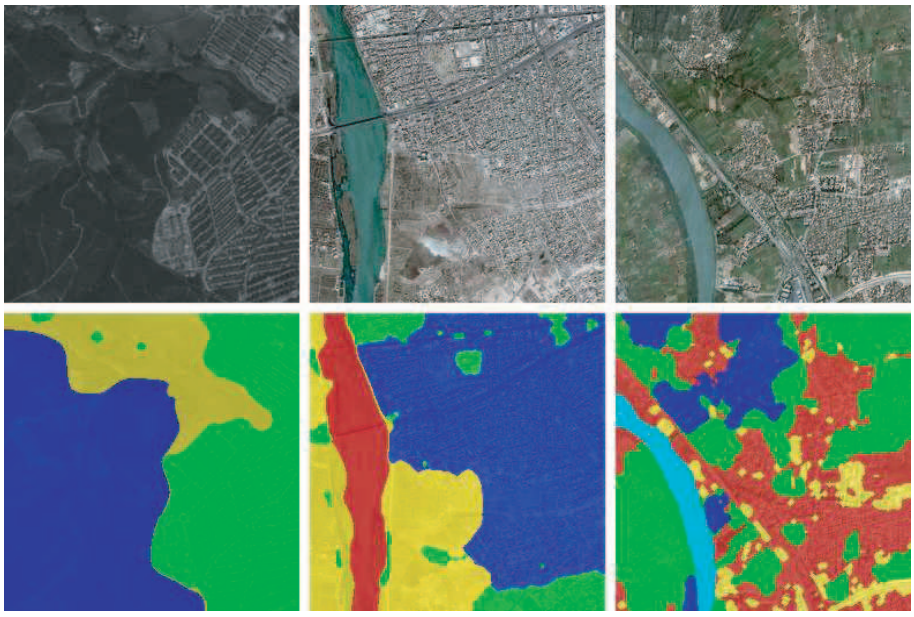

Figure 6: FROM LEFT TO RIGHT, TOP TO BOTTOM: (a), (b) and (c) Original images (256x256) containing both non-textured and textured regions. (d), (e) and (f) their corresponding segmentation results superimposed on original images.

4 Experimental Results

We first tested the performance of our method on natural images. Figure 3 shows typical segmentation results obtained respectively with an image without textured regions (3a), an image with only textured regions (3c) and two images containing both kinds of regions (3e,3g). In all the cases, the regions are separated from each other thanks to adaptive cues combination of color and texture.
An interesting application of our method is satellite images segmentation. Combining cues of spectral and texture according to their discrimination power provides a powerful framework to cope with satellite images. We applied our algorithm on various panchromatic and multispectral images acquired by SPOT-3 (4c), SPOT-5 (4a,5a,6a), IKONOS (6c) and QuickBird (4b,5b, 5c, 6b) satellites. Results for images without texture are illustrated in figure 4. Smooth regions like sea, agricultural area, urban in low resolution, green area and ground are cleanly segmented. Figure 5 shows segmentation results for textured region images. Urban with different densities, vegetation area and ground are well segmented. Finally, figure 6 illustrates the capabilities of our approach on images which contain both non-textured regions (eg. agricultural areas, ground, river) and textured regions (eg. mountains, urban).

5 Conclusion

In this paper, we have presented an adaptive variational segmentation method for satellite images. It is based on combining cues of spectral and texture according to their discrimination power for each region. Two weights, motivated by Fisher-Rao's linear discriminant analysis, are defined to code respectively the relevance of spectral and texture cues. Therefore, regions with or without texture are processed in the same framework. Promising results have been obtained on various natural images as well as on different satellite images.
In a future work, we intend to use the constructed nonlinear scale-space to provide a multiscale satellite images segmentation. Our aim is to decompose satellite image content into a hierarchy of attributed regions describing semantically topological relations and properties.

A The Weight's Gâteaux Derivative

The Gâteaux derivative of the spectral weight w_{1s} in the direction of V is:

$$\left\langle \left(w_{1s}\right)^{'}, V\right\rangle = \frac{1}{\sum_{j=1}^{M} Z_j}\left[w_{1t}\sum_{j=1}^{C}\left\langle Z_j^{'}, V\right\rangle - w_{1s}\sum_{j=C+1}^{M}\left\langle Z_j^{'}, V\right\rangle\right], \tag{31}$$

where $\mathrm{Z}_j = \frac{(\mu_{1j}-\mu_{2j})^2}{\left(\sigma_{1j}^2+\sigma_{2j}^2\right)}$. The Gâteaux derivative of $\mathrm{Z_j}$ in the of V is :

$$\left\langle Z_j', V\right\rangle = \int_{R_{\overrightarrow{\gamma}_1}}\left[\frac{Z_j}{|R_1|}\right]^{sh} dx - \int_{\overrightarrow{\gamma}_1}\frac{Z_j}{|R_1|}(V(x).N_1(x))da(x) \tag{32}$$

Using the following equalities :

$$\begin{cases} \left\langle |R_i|^{'}, V\right\rangle = -/+\int_{\overrightarrow{\gamma}_1}\left(V\left(x\right).N_1\left(x\right)\right)da\left(x\right) \\ \left\langle \left(\mu_{ij}\right)^{'}, V\right\rangle = -/+\frac{1}{|R_i|}\int_{\overrightarrow{\gamma}_1}\left(\mathbf{U}_j\left(x\right)-\mu_{ij}\right)\left(V\left(x\right).N_1\left(x\right)\right)da\left(x\right) \\ \left\langle \left(\sigma_{ij}^2\right)^{'}, V\right\rangle = -/+\frac{1}{|R_i|}\int_{\overrightarrow{\gamma}_1}\left(\left(\mathbf{U}_j\left(x\right)-\mu_{ij}\right)^2-\sigma_{ij}^2\right)\left(V\left(x\right).N_1\left(x\right)\right)da\left(x\right), \end{cases} \tag{33}$$

we obtain:

$$\begin{aligned} \left\langle Z_j', V\right\rangle &= \sum_{i=1}^{2}\left(\frac{\partial Z_j}{\partial \mu_{ij}}\left\langle \left(\mu_{ij}\right)^{'}, V\right\rangle + \frac{\partial Z_j}{\partial \sigma_{ij}^2}\left\langle \left(\sigma_{ij}^2\right)^{'}, V\right\rangle\right) \\ &= \int_{\overrightarrow{\gamma}_1} k_{1j}\left(x\right)\left(V\left(x\right).N_1\left(x\right)\right)da\left(x\right), \end{aligned} \tag{34}$$

where

$$\begin{aligned} k_{1j}\left(x\right) &= 2\frac{\left(\mu_{2j}-\mu_{1j}\right)}{\left(\sigma_{1j}^2+\sigma_{2j}^2\right)}\left(\frac{\left(U_j(x)-\mu_{1j}\right)}{|R_1|}+\frac{\left(U_j(x)-\mu_{2j}\right)}{|R_2|}\right) \\ &+\frac{\left(\mu_{1j}-\mu_{2j}\right)^2}{\left(\sigma_{1j}^2+\sigma_{2j}^2\right)^2}\left(\frac{\left(U_j(x)-\mu_{1j}\right)^2-\sigma_{1j}^2}{|R_1|}-\frac{\left(U_j(x)-\mu_{2j}\right)^2-\sigma_{2j}^2}{|R_2|}\right) \end{aligned} \tag{35}$$

Then, the Gâteaux derivative of w_{1s} in the direction of V is:

$$\left\langle \left(w_{1s}\right)^{'}, V\right\rangle = \frac{1}{\sum_{j=1}^{M} Z_j}\int_{\overrightarrow{\gamma}_1}\left[w_{1t}\sum_{j=1}^{C}k_{1j}(x) - w_{1s}\sum_{j=C+1}^{M}k_{1j}(x)\right](V(x).N_1(x))\,da(x) \tag{36}$$

B Generalization to N Regions

For N regions image segmentation, we have $Z_{1j} = \frac{\sum_{i=1}^{N} (\mu_{1j} - \mu_{ij})^2}{\sum_{i=1}^{N} \sigma_{ij}^2}$ and its Gâteaux derivative is:

$$\left\langle (Z_{1j})', V \right\rangle = \sum_{i=1}^{N} \left(\frac{\partial Z_{1j}}{\partial \mu_{ij}} \left\langle (\mu_{ij})', V \right\rangle + \frac{\partial Z_{1j}}{\partial \sigma_{ij}^2} \left\langle (\sigma_{ij}^2)', V \right\rangle \right) \tag{37}$$

Using the following equalities :

$$\frac{\partial Z_{1j}}{\partial \mu_{1j}} = \frac{2 \sum_{i=2}^{N} (\mu_{1j} - \mu_{ij})}{\sum_{i=1}^{N} \sigma_{ij}^2}, \ \frac{\partial Z_{1j}}{\partial \mu_{kj}}\Big|_{k\in[2,N]} = \frac{-2 (\mu_{1j} - \mu_{kj})}{\sum_{i=1}^{N} \sigma_{ij}^2}, \ \frac{\partial Z_{1j}}{\partial \sigma_{kj}^2}\Big|_{k\in[1,N]} = -\frac{\sum_{i=1}^{N} (\mu_{1j} - \mu_{ij})^2}{\left(\sum_{i=1}^{N} \sigma_{ij}^2 \right)^2} \tag{38}$$

$$\begin{array}{l} \left\langle (\mu_{1j})', V \right\rangle = -\frac{1}{|R_1|} \int_{\overrightarrow{\gamma}_1} (\mathbf{U}_j(x) - \mu_{1j})(V(x) . N_1(x)) \, da(x) \\ \left\langle (\mu_{kj})', V \right\rangle\Big|_{k\in[2,N]} = \frac{1}{|R_k|} \int_{\overrightarrow{\gamma}_1} (\mathbf{U}_j(x) - \mu_{kj}) \chi_k^1(x)(V(x) . N_1(x)) \, da(x) \\ \left\langle (\sigma_{1j}^2)', V \right\rangle = -\frac{1}{|R_1|} \int_{\overrightarrow{\gamma}_1} \left((\mathbf{U}_j(x) - \mu_{1j})^2 - \sigma_{1j}^2 \right) (V(x) . N_1(x)) \, da(x) \\ \left\langle (\sigma_{kj}^2)', V \right\rangle\Big|_{k\in[2,N]} = \frac{1}{|R_k|} \int_{\overrightarrow{\gamma}_1} \left((\mathbf{U}_j(x) - \mu_{kj})^2 - \sigma_{kj}^2 \right) \chi_k^1(x)(V(x) . N_1(x)) \, da(x) \end{array} \tag{39}$$

we have:

$$\left\langle Z_{1j}', V \right\rangle = \int_{\overrightarrow{\gamma}_1} k_{1j}^1(x) \left(V(x) . N_1(x) \right) da(x), \tag{40}$$

where

$$\begin{array}{rl} k_{1j}^1(x) & = \frac{-2}{\sum_{i=1}^{N} \sigma_{ij}^2} \sum_{k=2}^{N} \left[(\mu_{1j} - \mu_{kj}) \left(\frac{\mathbf{U}_j(x) - \mu_{1j}}{|R_1|} + \frac{\mathbf{U}_j(x) - \mu_{kj}}{|R_k|} \chi_k^1(x) \right) \right] \\ & + \frac{\sum_{i=1}^{N} (\mu_{1j} - \mu_{ij})^2}{\left(\sum_{i=1}^{N} \sigma_{ij}^2 \right)^2} \left[\frac{(\mathbf{U}_j(x) - \mu_{1j})^2 - \sigma_{1j}^2}{|R_1|} - \sum_{k=2}^{N} \left(\frac{(\mathbf{U}_j(x) - \mu_{kj})^2 - \sigma_{kj}^2}{|R_k|} \chi_k^1(x) \right) \right] \end{array} \tag{41}$$

Then, the Gâteaux derivative of w_{1s} in the direction of V is:

$$\left\langle (w_{1s})', V \right\rangle = \frac{1}{\sum_{j=1}^{M} Z_{1j}} \int_{\overrightarrow{\gamma}_1} \left[w_{1t} \sum_{j=1}^{C} k_{1j}^1(x) - w_{1s} \sum_{j=C+1}^{M} k_{1j}^1(x) \right] (V(x) . N_1(x)) \, da(x) \tag{42}$$

Therefore, we get the following region functional Gâteaux derivative:

$$\left\langle D' \left(R_{\overrightarrow{\gamma}_1} \right), V \right\rangle = \int_{\overrightarrow{\gamma}_1} \left[A_1 \left(w_{1t} \sum_{j=1}^{C} k_{1j}^1(x) - w_{1s} \sum_{j=C+1}^{M} k_{1j}^1(x) \right) - \xi_1(x) \right] (V(x) . N_1(x)) \, da(x) \tag{43}$$

where $A_1 = \frac{|R_1|\left((2C-M)(1+\log(2\Pi))+\sum_{j=1}^{C}\log\left(\sigma_{1j}^2\right)-\sum_{j=C+1}^{M}\log\left(\sigma_{1j}^2\right)\right)}{\sum_{j=1}^{M} Z_{1j}}$.

As the same, we compute the Gâteaux derivative of $D\left(R^c_{\overrightarrow{\gamma}_1}\right)$. Since $\left\langle D'\left(R^c_{\overrightarrow{\gamma}_1}\right), V\right\rangle = \sum_{i=2}^{N}\int_{R_{\overrightarrow{\gamma}_1}}\left[\xi_i(x)\,\chi_i(x)\right]^{sh}dx + \int_{\overrightarrow{\gamma}_1}\Phi_1(x)(V(x).N_1(x))\,da(x)$, then this derivative can be expressed as:

$$\left\langle D'\left(R^c_{\overrightarrow{\gamma}_1}\right), V\right\rangle = \int_{\overrightarrow{\gamma}_1}\left[\sum_{i=2}^{N}A_i\left(w_{it}\sum_{j=1}^{C}k_{ij}^1(x) - w_{is}\sum_{j=C+1}^{M}k_{ij}^1(x)\right)+\Phi_1(x)\right](V(x).N_1(x))\,da(x), \tag{44}$$

where for $i=2,\ldots,N$, $A_i = \frac{|R_i|\left((2C-M)(1+\log(2\Pi))+\sum_{j=1}^{C}\log\left(\sigma_{ij}^2\right)-\sum_{j=C+1}^{M}\log\left(\sigma_{ij}^2\right)\right)}{\sum_{j=1}^{M} Z_{ij}}$ and

$$\begin{aligned} k_{ij}^1(x) &= \frac{2\left(\mu_{ij}-\mu_{1j}\right)}{\sum_{k=1}^{N}\sigma_{kj}^2}\left(\frac{\mathbf{U}_j(x)-\mu_{ij}}{|R_i|}\chi_i^1(x)+\frac{\mathbf{U}_j(x)-\mu_{1j}}{|R_1|}\right) \\ &+\frac{2}{\sum_{k=1}^{N}\sigma_{kj}^2}\sum_{k=2}^{N}\left[\left(\mu_{ij}-\mu_{kj}\right)\left(\frac{\mathbf{U}_j(x)-\mu_{ij}}{|R_i|}\chi_i^1(x)-\frac{\mathbf{U}_j(x)-\mu_{kj}}{|R_k|}\chi_k^1(x)\right)\right] \\ &+\frac{\sum_{k=1}^{N}\left(\mu_{ij}-\mu_{kj}\right)^2}{\left(\sum_{k=1}^{N}\sigma_{kj}^2\right)^2}\left[\frac{\left(\mathbf{U}_j(x)-\mu_{1j}\right)^2-\sigma_{1j}^2}{|R_1|}-\sum_{k=2}^{N}\left(\frac{\left(\mathbf{U}_j(x)-\mu_{kj}\right)^2-\sigma_{kj}^2}{|R_k|}\chi_k^1(x)\right)\right] \end{aligned} \tag{45}$$

References

[1] A. W. M. Smeulders, M. Worring, S. Santini, A. Gupta, and R. Jain. Content-based image retrieval at the end of the early years. *IEEE Transactions on Pattern Analysis and Machine Intelligence*, 22(12):1349–1380, 2000.

[2] J. A. Sethian. *Level set methods and fast marching methods.* Cambridge University Press, 1999.

[3] N. Paragios and R. Deriche. Geodesic active regions and level set methods for supervised texture segmentation. *International Journal of Computer Vision*, 46(3):223–247, 2002.

[4] M. Rousson and R. Deriche. A variational framework for active and adaptive segmentation of vector valued images. In *IEEE Workshop on Motion and Video Computing*, pages 56–61, Orlando, Florida, 2002.

[5] T. Brox, M. Rousson, R. Deriche, and J. Weickert. Unsupervised segmentation incorporating colour, texture and motion. Technical Report 4760, INRIA, March 2003.

[6] A.-R. Mansouri, A. Mitiche, and C. Vazquez. Image partitioning by level set multiregion competition. In *IEEE International Conference on Image Processing*, pages 2721–2724, October 2004.

[7] J. Malik, S. Belongie, T. Leung, and J. Shi. Contour and texture analysis for image segmentation. *International Journal of Computer Vision*, 43(1):7–27, June 2001.

[8] Y. Deng and B. S. Manjunath. Unsupervised segmentation of color-texture regions in images and video. *IEEE Transactions on Pattern Analysis and Machine Intelligence*, 23(8):800–810, 2001.

[9] W. Ma and B. Manjunath. EdgeFlow: a technique for boundary detection and image segmentation. *IEEE Transactions on Image Processing*, 9(8):1375–88, August 2000.

[10] B. Sumengen, B. S. Manjunath, and C. Kenney. Image segmentation using curve evolution and flow fields. In *IEEE International Conference on Image Processing*, pages 105–108, September 2002.

[11] J. F. Aujol and T. F. Chan. Combining geometrical and textured information to perform image classification. In *3nd IEEE Workshop on Variational, Geometric and Level Set Methods in Computer Vision*, pages 161–172, Beijing, October 2005.

[12] C. Sagiv, N. A. Sochen, and Y. Y. Zeevi. Texture segmentation via a diffusion segmentation scheme in the gabor feature space. In *2nd International Workshop on Texture Analysis and Synthesis*, Copenhagen, June 2002.

[13] B. Sandberg, T. Chan, and L. Vese. A level-set and gabor-based active contour algorithm for segmenting textured images. Technical Report 39, Math. Dept. UCLA, Los Angeles, USA, July 2002.

[14] T. Brox and J. Weickert. A TV flow based local scale measure for texture discrimination. In *8th European Conference on Computer Vision*, volume 2, pages 578–590, Parague, May 2004.

[15] T. Brox and J. Weickert. Level set based image segmentation with multiple regions. *Pattern Recognition*, 3175:415–423, August 2004.

[16] J. Weickert, B. M. Romeny, and M. A. Viergever. Efficient and reliable schemes for nonlinear diffusion filtering. *IEEE Transactions on Image Processing*, 7(3):398–410, March 1998.

[17] R. A. Fisher. The statistical utilization of multiple measurements. *Annals of Eugenics*, 8:376–386, 1938.

[18] C. R. Rao. The utilization of multiple measurements in problems of biological classification. *Journal of the Royal Statistical Society*, 10(B):159–203, 1948.

[19] M. Loog, R. P. W. Duin, and R. Haeb-Umbach. Multiclass linear dimension reduction by weighted pairwise Fisher criteria. *IEEE Transactions on Pattern Analysis and Machine Intelligence*, 23(7):762–766, 2001.

[20] S. Mika, G. Rätsch, J. Weston, B. Schölkopf, and K.-R. Müller. Constructing descriptive and discriminative nonlinear features: Rayleigh coefficients in kernel feature spaces. *IEEE Transactions on Pattern Analysis and Machine Intelligence*, 25(5):623–628, May 2003.

[21] J. Yang, A. F. Frangi, J. Y. Yang, D. Zhang, and Z. Jin. KPCA plus LDA: A complete kernel Fisher discriminant framework for feature extraction and recognition. *IEEE Transactions on Pattern Analysis and Machine Intelligence*, 27(2):230–244, February 2005.

[22] C. Samson, L. Blanc-Féraud, G. Aubert, and J. Zerubia. A level set model for image classification. *International Journal of Computer Vision*, 40(3):187–197, Mars 2000.

[23] G. Aubert, M. Barlaud, O. Faugeras, and S. Jehan-Besson. Image segmentation using active contours: Calculus of variations of shape gradients? *SIAM Journal on Applied Mathematics*, 63(6):2128–2154, 2003.

Unité de recherche INRIA Rocquencourt
Domaine de Voluceau - Rocquencourt - BP 105 - 78153 Le Chesnay Cedex (France)

Unité de recherche INRIA Futurs : Parc Club Orsay Université - ZAC des Vignes
4, rue Jacques Monod - 91893 ORSAY Cedex (France)
Unité de recherche INRIA Lorraine : LORIA, Technopôle de Nancy-Brabois - Campus scientifique
615, rue du Jardin Botanique - BP 101 - 54602 Villers-lès-Nancy Cedex (France)
Unité de recherche INRIA Rennes : IRISA, Campus universitaire de Beaulieu - 35042 Rennes Cedex (France)
Unité de recherche INRIA Rhône-Alpes : 655, avenue de l'Europe - 38334 Montbonnot Saint-Ismier (France)
Unité de recherche INRIA Sophia Antipolis : 2004, route des Lucioles - BP 93 - 06902 Sophia Antipolis Cedex (France)

Éditeur
INRIA - Domaine de Voluceau - Rocquencourt, BP 105 - 78153 Le Chesnay Cedex (France)
http://www.inria.fr
ISSN 0249-6399